Response to Anonymous Referee #1

We are grateful to the Anonymous Referee #1 for the detailed comments and suggestions which greatly improved the quality of our manuscript. Our manuscript has been revised according to the comments from the Referee and our responses to the comments are as follows. Reviewer comments have been copied (R:) and replied to (A:) below. For clarity, the comments are reproduced in blue, authors' responses are in black and changes in the manuscript are in red.

General comments:

This manuscript investigated the SOA formation from a mixture of α-pinene and DMS in laboratory chamber experiments. It is found that DMS has a non-linear effect on SOA generation: the mass concentration and yield of SOA show an increasing and then decreasing trend with the increase of the initial concentration of DMS. Potential interaction mechanisms have been proposed. Detailed offline characterization of SOA composition was conducted and utilized to investigate the SOA formation mechanism. However, the analysis has fundamental flaws. I cannot recommend publication in its current form.

Major comments:

R1-1:) The SOA yield is a function of existing organic aerosol (delta_Mo) (Pankow, 1994). This fundamental concept is key in explaining the observed results, but is completely ignored throughout the discussion.

A1-1:) Thank you for your valuable suggestion. As you said, establishing a functional relationship between SOA yield and existing organic aerosol (ΔMo) is key to interpreting the experimental results. We have added a series of experiments to establish a quantitative relationship between SOA yield and ΔMo for either α-pinene or DMS, as shown in Tables R1 and R2 below. All experiments were conducted at temperature of 299 ± 1 K and relative humidity (RH) of 30 – 40%. The corresponding contents are added in the revised manuscript (Page 10, Lines 216-217) and supplement (SI Pages 3-4, Lines 48-58; SI Page 20, Lines 291-294).

Table R1. Complementary experiments on the oxidation of individual α-pinene.

Exp. No.	$[\alpha\text{-pinene}]_0$ ppb	$\Delta[\alpha\text{-pinene}]$ ppb	$[NO]_0$ ppb	$[NO_x]_0$ ppb	[SOA] μg m^{-3}	Y
A'-1	111	111	186	197	73.8	0.12±0.01
A'-2	199	199	196	205	191.8	0.17±0.02
A'-3	317	317	203	211	269.6	0.15±0.02
A'-4	415	415	199	207	410.7	0.18±0.02
A'-5	506	506	174	186	830.8	0.30±0.03

Table R2. Complementary experiments on the oxidation of individual DMS.

Exp. No.	$[DMS]_0$ ppb	Δ[DMS] ppb	$[NO]_0$ ppb	$[NO_x]_0$ ppb	[Total particles] μg m^{-3}	$[H_2SO_4]$ μg m^{-3}	[MSA] μg m^{-3}	[SOA] μg m^{-3}	Y
D'-1	90	90	207	215	50.5	11.0	8.0	22.0	0.09±0.01
D'-2	161	159	198	207	171.1	43.5	55.2	85.9	0.21±0.02
D'-3	275	275	199	209	599.7	98.9	39.9	278.1	0.40±0.04
D'-4	292	265	212	222	556.9	97.4	150.2	295.6	0.44±0.04

A semi-empirical model based on gas-particle partitioning can be used to describe the relationship between yield and mass loading (Odum et al., 1996; Pankow, 1994), which can be expressed by the following equation (R1):

$$Y=M_O\sum_i \frac{\alpha_i K_{om,i}}{1+K_{om,i}M_O} \quad (R1)$$

where α_i and $K_{om,\,i}$ (m^3 μg^{-1}) are the mass-based gas-phase stoichiometric fraction and gas-particle partitioning coefficient, respectively. Y is the SOA yield, and ΔM_O is the formed SOA mass concentration. In this model, it is generally assumed that the VOC is converted into a higher volatility product and a lower volatility product. The relationship curve between SOA mass concentration and yield in the experiment can be obtained by fitting the semi-empirical model. The parameters of the base group with lower product volatility were also calculated as α_1, $K_{om,\,1}$, and the parameters of the base group with higher volatility are α_2, $K_{om,\,2}$.

The fitted curves are shown in Fig. R1 below. The DMS fitting curves were also plotted including Exp. D-1. For the individual oxidation experiments of α-pinene, the parameters were as follows: R^2_A = 0.99, $\alpha_{1,\,A}$ = 0.630, $K_{om,\,1,\,A}$ = 5.178 × 10^{-4}, $\alpha_{2,\,A}$ = 0.0951, $K_{om,\,2,\,A}$ = 0.0624. For DMS, the parameters were as follows: R^2_D = 0.99, $\alpha_{1,\,D}$ = 1.076, $K_{om,\,1,\,D}$ = 0.00141, $\alpha_{2,\,D}$ = 0.111, $K_{om,\,2,\,D}$ = 0.0623. The M_O-dependent SOA yields of α-pinene and DMS were also used to calculate the predicted SOA mass concentration in the mixed experiments, **see our response to Comment R1-3.**

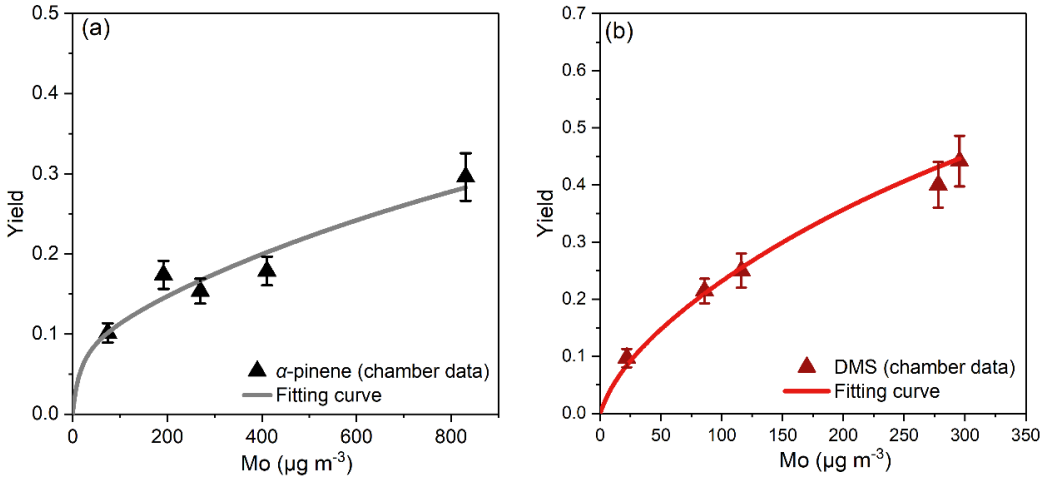

Figure R1. Mass-dependent SOA yields for the oxidation of α-pinene (a) and DMS (b), individually.

We have also added relevant text in the revised manuscript. As follows:

"A semi-empirical model based on gas-particle partitioning can be used to describe the relationship between yield and mass loading (Odum et al., 1996; Pankow, 1994). The calculation process is shown in Sect. S3 in the supplement. Experiments for both individual α-pinene and individual DMS were simulated using this model. The complementary experiments for the two VOCs are shown in Tables S2 and S3. The DMS fitting curves were also plotted including Exp. D-1. The fitted curves are shown in Fig. 3. For the individual oxidation experiments of α-pinene, the parameters were as follows: $R^2_A = 0.99$, $\alpha_{1,A} = 0.630$, $K_{om,1,A} = 5.178 \times 10^{-4}$, $\alpha_{2,A} = 0.0951$, $K_{om,2,A} = 0.0624$. For DMS, $R^2_D = 0.99$, $\alpha_{1,D} = 1.076$, $K_{om,1,D} = 0.00141$, $\alpha_{2,D} = 0.111$, $K_{om,2,D} = 0.0623$." (Pages 9-10, Lines 201-207)

R1-2:) In Fig. 2, there is clear difference between measured and modeled DMS, but this issue is not discussed in the manuscript. The difference is surprising given the α-pinene decay is reasonably modeled. Perhaps the DMS measurement has issues. Further, the difference challenges the reliability of modeling results (e.g., Figure 2) and any conclusions drawn based on modeling.

A1-2:) Thank you for your valuable suggestion. First, we think that the DMS measurement is accurate. In our experiments, DMS was detected using GC-FID. We utilized the area of peak at 1.37-1.5 min to quantify DMS, and the calibration curve is shown in Fig. R2 below. There is a good linear correlation between the peak area and the DMS concentration ($R^2 = 0.991$).

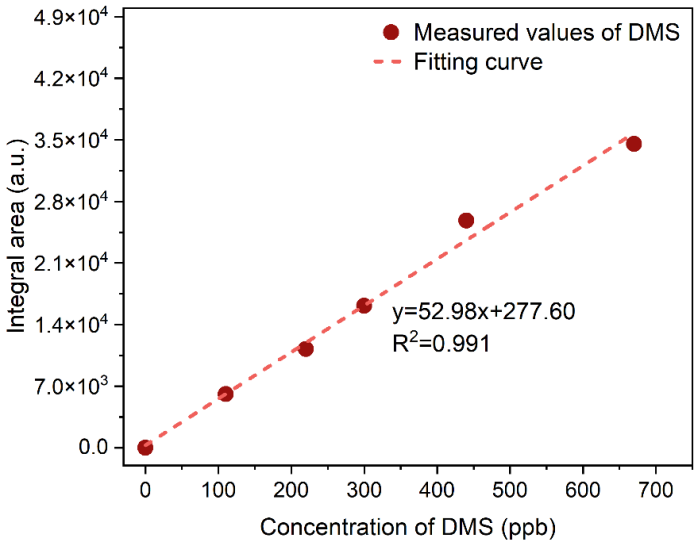

Figure R2. Calibration curve of DMS concentration.

Secondly, the large difference between the measured DMS and the modeled DMS is observed in the mixed experiments. This is likely due to the incompleteness of the MCM model for the oxidation mechanism of DMS. We have mentioned the difference in the revised supplement. We elaborate on this reason here as well. The imperfection of the DMS oxidation mechanism in the model and the fact that most studies only focus

on the oxidation mechanism of individual species and lack the mechanism of interaction from the overall perspective result in incomplete agreement of the model simulations (Coates and Butler, 2015; Knote et al., 2015; Zong et al., 2018; Yang et al., 2022). In addition, the MCM DMS scheme suffers from a number of problems. Firstly, unlike the other VOCs simulated by the MCM (alkanes, alkenes, aromatics, and oxygenates), the DMS scheme has rarely evaluated against chamber experiments. We have incorporated the oxidation mechanism of autoxidation of $CH_3SCH_2O_2$ into the MCM model (Table R3) (Berndt et al., 2020; Ye et al., 2022; Jernigan et al., 2022; Lv et al., 2019; Jacob et al., 2024; Chen et al., 2021; Berndt et al., 2023; Veres et al., 2020; Assaf et al., 2023). However, the MCM DMS scheme is rather outdated (Jacob et al., 2024). In addition, the uncertainty in the gas-phase reaction rate constants of the products of DMS and DMS (Chen and Jang, 2012). The corresponding contents are added in the revised supplement (SI Page 5, Lines 93-102; SI Pages 22-23, Line 300).

Table R3. Mechanisms related to DMS added to the MCM model.

Reaction	**Rate constant**
$CH_3SCH_2O_2$ = $HOOCH_2SCH_2O_2$	$2.39\times10^{9}\times e^{-7278/T}$
$HOOCH_2SCH_2O_2$ = HPMTF + OH	$6.10\times10^{11}\times e^{-9.5\times10\text{^}3/T+1.1\times10\text{^}8/T\text{^}3}$
$HOOCH_2SCH_2O_2$ + NO = $HOOCH_2SCH_2O$ + NO_2	$4.90\times10^{-12}\times e^{260/T}$
$HOOCH_2SCH_2O_2$ + HO_2 = $HOOCH_2SCH_2OOH$	KRO2HO2×0.387
$HOOCH_2SCH_2O_2$ + NO_3 = $HOOCH_2SCH_2O$ + NO_2	KRO2NO3
$HOOCH_2SCH_2O_2$ = $HOOCH_2SCH_2O$	$3.74\times10^{-12}\times[RO_2]\times0.8$
$HOOCH_2SCH_2O_2$ = $HOOCH_2SCH_2OH$	$3.74\times10^{-12}\times[RO_2]\times0.91$
$HOOCH_2SCH_2O_2$ = HPMTF	$3.74\times10^{-12}\times[RO_2]\times0.09$
$HOOCH_2SCH_2O$ = $HOOCH_2S$ + HCHO	1.00×10^{6}
HPMTF + OH = $HOOCH_2S$ + CO	$1.75\times10^{-11}\times0.91$
HPMTF + OH = OH + HCHO + OCS	$1.75\times10^{-11}\times0.09$
HPMTF = $HOOCH_2S$ + HO_2 + CO	2.10×10^{-11}
$HOOCH_2SCH_2OH$ + OH = HPMTF + HO_2	2.78×10^{-11}
$HOOCH_2SCH_2OOH$ + OH = $HOOCH_2SCH_2O_2$	$2.00\times3.68\times10^{-13}\times e^{635/T}$
OCS + O = CO + SO	$2.10\times10^{-11}\times e^{-2200/T}$
OCS + OH = SO + OH	$7.20\times10^{-14}\times e^{-1070/T}$
SO = SO_2 + O	$1.60\times10^{-13}\times e^{-2280/T}\times[O_2]$
SO + O_3 = SO_2	$3.40\times10^{-12}\times e^{-1100/T}$
SO + NO_2 = SO_2 + NO	1.40×10^{-11}
SO + OH = SO_2 + HO_2	$2.60\times10^{-11}\times e^{330/T}$
$HOOCH_2S$ + O_3 = $HOOCH_2SO$	$1.50\times10^{-12}\times e^{360/T}$
$HOOCH_2S$ + NO_2 = $HOOCH_2SO$ + NO	$3.00\times10^{-11}\times e^{240/T}$
$HOOCH_2S$ = $HOOCH_2SOO$	$1.20\times10^{-16}\times e^{1580/T}\times[O_2]$
$HOOCH_2SOO$ = TPA + HO_2	$7.13\times10^{-31}\times T^{14.02}\times e^{-2556/T}$
$HOOCH_2SOO$ = $HOOCH_2S$	1.50×10^{5}
$HOOCH_2SOO$ = SO_2 + HCHO + OH	5.00
TPA + OH = OCS + OH	$5.00\times10^{-11}\times0.14$
TPA + OH = OCHSOH + OH	$5.00\times10^{-11}\times0.86$

Reaction	Rate constant
$OCHSOH + OH = OCS + OH$	1.40×10^{-12}
$HOOCH_2SO + O_3 = SO_2 + HCHO + OH$	4.00×10^{-13}
$HOOCH_2SO + NO_2 = SO_2 + HCHO + OH + NO$	1.20×10^{-11}
$OCH_2SCH_2OH = HOCH_2S + HCHO$	1.00×10^{6}
$HOCH_2S + O_3 = HOCH_2SO$	$1.50\times10^{-12}\times e^{360/T}$
$HOCH_2S + NO_2 = HOCH_2SO + NO$	$3.00\times10^{-11}\times e^{240/T}$
$HOCH_2S = HOCH_2SOO$	$1.20\times10^{-16}\times e^{1580/T}\times[O_2]$
$HOCH_2SOO = HOCH_2S$	1.50×10^{5}
$HOCH_2SOO = SO_2 + HCHO + HO_2$	5.00
$HOCH_2SO + O_3 = SO_2 + HCHO + HO_2$	4.00×10^{-13}
$HOCH_2SO + NO_2 = SO_2 + HCHO + HO_2 + NO$	1.20×10^{-11}
$OCH_2SCHO = HCHO + OCS + HO_2$	1.00×10^{6}

The following texts were also added in the revised manuscript.

"We have also added the reaction equations and rates obtained from previous studies on the isomerization reaction of the DMS-generated $CH_3SCH_2O_2$ radical (Berndt et al., 2020; Ye et al., 2022; Jernigan et al., 2022; Lv et al., 2019; Jacob et al., 2024; Chen et al., 2021; Berndt et al., 2023; Veres et al., 2020; Assaf et al., 2023) (Table S5)." (Page 7, Lines 167–170)

"In addition, we also fitted the consumption trends of VOCs with the MCM model. There is some deviation between the measured DMS and the fitted DMS in mixed systems. The reasons for the deviation are detailed in Sect. S5 of the supplement. The time series of inorganic gases and the related presentation of the connection with SOA formation are also presented in Sect. S5 of the supplement." (Pages 8-9, Lines 194–197)

Thirdly, the results presented in Fig. 2 of the original manuscript (now Fig. 4c, d in the revised manuscript) are all measured results rather than modeled results. We presented the calculation of average OH concentration and OH reactivity in the supplement (Sect. S6 on Page 6). We have added the relevant texts in the manuscript as well. As follows:

"$[OH]_{avg}$ and OHR were estimated from experimental measurements of VOC concentrations and their OH reaction rate constants. Detailed calculations are given in Sect. S6." (Page 11, Lines 231-233)

Overall, the use of MCM is only supportive. We use this model for the purpose of getting the trend of OH changes in different systems. The vast majority of the results in the manuscript are measured. Although MCM mechanism of DMS is not well established, we believe that the modelled reactivity trend could be used for the comparison with measurements and therefore provide some hints.

R1-3:) The first paragraph under section 2. The effect of α-pinene + DMS interaction on SOA yield should be systematically evaluated for all experiments and illustrated graphically. It is not sufficient to compare one set of experiments only in words. Also,

an alternative and more meaningful way is to compare [delta α-pinene] * SOA yield$_{\alpha\text{-pinene}}$ + [delta DMS] * SOA yield$_{DMS}$ vs SOA mass formed in the mixed experiments. The SOA yields should correspond to the total SOA mass in the mixed experiments.

A1-3:) Thank you for your valuable suggestion. We calculated the predicted mass concentration for mixed experiments as shown in equations (R2) and (R3) below:

$$\Delta M_i = \Delta VOC_i Y_i \quad (R2)$$

$$\Delta M_o = \sum_{i=1}^{n} \Delta M_i \quad (R3)$$

where Y_i denotes the predicted value calculated using the semi-empirical model when the value of ΔM_O is equal to that of the mixed experiments, for both α-pinene and DMS. ΔVOC_i (μg m^{-3}) denotes the consumption of α-pinene or DMS in the mixed system (Exp. AD-3). ΔM_i denotes the corresponding predicted mass concentrations of the two VOCs (μg m^{-3}), and ΔM_0 denotes the sum of the predicted mass concentrations of the mixed VOCs (μg m^{-3}).

A comparison of the predicted and measured mass concentration were shown in Fig. R3 below. Consistent with the measured values, the predicted SOA mass concentration showed a turning point at Δ[DMS]/Δ[α-pinene] of 1.097. The measured SOA mass concentration was greater than predicted SOA mass concentration for Δ[DMS]/Δ[α-pinene] below 1.056. In this ratio range, DMS promoted the generation of SOA in the mixed systems. When the ratio was higher than 1.056, the measured SOA mass concentration was lower than the predicted SOA mass concentration, indicating a possible inhibition effect. The corresponding contents are added in the revised manuscript (Page 10, Lines 210-215) and revised supplement (SI Page 4, Lines 59-63).

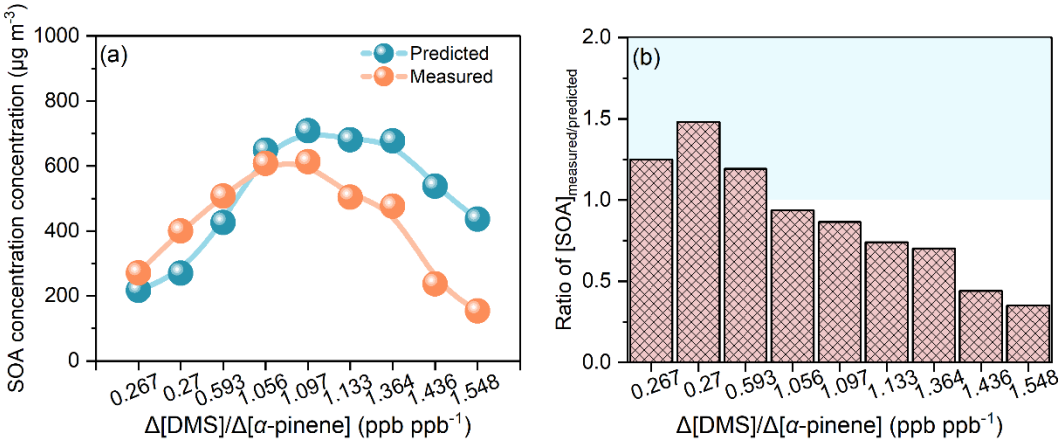

Figure R3. Comparison of predicted and measured SOA mass concentration in mixed systems. (a) Measured and predicted SOA mass concentrations in different mixed experiments. (b) Ratio of measured to predicted SOA mass concentration.

The following texts in Table 2 were added in the revised manuscript (Page 9, Line 198).

Table 2. Experimental results of particle-phase components in photooxidation of DMS/α-pinene/NO_x systems.

Exp. No.	[Total particles] [a] μg m^{-3}	[H_2SO_4][b] μg m^{-3}	[MSA][b] μg m^{-3}	[SOA_m][c] μg m^{-3}	Y_m[d]	[SOA_p][e] μg m^{-3}
individual α-pinene						
A-1	269.5	-	-	269.5	0.16±0.02	
individual DMS						
D-1	177.2	50.8	32.83	116.2	0.25±0.03	
mix α-pinene and DMS						
AD-1	296.3	15.0	22.2	270.8	0.14±0.02	216.7
AD-2	422.3	15.7	22.5	400.1	0.20±0.02	270.3
AD-3	572.6	45.4	24.9	507.5	0.24±0.02	425.8
AD-4	714.4	55.4	50.5	607.7	0.25±0.03	648.7
AD-5	683.0	48.8	36.2	613.1	0.24±0.02	708.2
AD-6	551.5	35.3	8.5	504.2	0.19±0.02	680.9
AD-7	539.9	48.4	16.8	476.0	0.19±0.02	677.5
AD-8	364.4	68.7	0.1	237.1	0.08±0.01	537.6
AD-9	289.9	83.2	7.0	154.0	0.06±0.01	436.5

[a] The mass concentration of particles generated by SMPS, corrected for particle wall loss, was calculated as a particle density of 1.2 g cm^{-3}.
[b] IC detection, particle-phase products generated by DMS photooxidation. NH_4^+ was hardly detected. All SO_4^{2-} were detected by IC as H_2SO_4.
[c] The measured SOA mass concentration is expressed as $[\text{Total particles}]_{\text{after-correction}} \times (1 - [H_2SO_4] / [\text{Total particles}]_{\text{before-correction}})$.
[d] $[SOA_m] / (\Delta[\alpha\text{-pinene}] + \Delta[\text{DMS}])$, as mixed yield. Error bars indicate SMPS instrument error of 10%.
[e] The predicted SOA mass concentration by using mass-dependent SOA yields of α-pinene and DMS.

We have also added additional texts to the revised manuscript regarding the calculation of predicted mass concentration:

"We evaluated the predicted mass concentration of SOA for two individual systems by using this model. The calculations took place under the condition that the existing organic aerosol (ΔMo) of the mixed system was equal to that of the individual system. The predicted mass concentration for the different mixed systems were calculated using equations (7) and (8) in the Sect. S3." (Page 10, Lines 207-210)

R1-4:) The proposed explanation regarding the effects of adding DMS on OH concentration is confusing. If the initial OH increase is because of OH regeneration from DMS oxidation, how could it be possible that further adding DMS will reduce OH?

A1-4:) Thank you for your valuable suggestion. The $CH_3SCH_2O_2$ radical generated from DMS oxidation reacts with NO, RO_2, and HO_2, and also undergoes isomerization reactions to form OH (Jacob et al., 2024; Berndt et al., 2023; Ye et al., 2022). We have

added reactions related to the isomerization pathway of the $CH_3SCH_2O_2$ radical to the MCM model, **see our answer to Comment R1-2 for details**.

We evaluate the absolute amount of the isomerization channel of the $CH_3SCH_2O_2$ radical using the MCM model. The corresponding contents are added in the revised manuscript (Page 12, Lines 267-272; Page 13, Lines 273-277, 284-286) and supplement (SI Pages 7-8, Lines 128-141). The parameters related to each reaction channel of the $CH_3SCH_2O_2$ radical generated by DMS oxidation were calculated as shown in equations (R4) - (R9):

$$v_{CH_3SCH_2O_2+X,t} = k_{CH_3SCH_2O_2+X}[X]_t \quad (R4)$$

$$C_{CH_3SCH_2O_2+X,t} = \frac{v_{CH_3SCH_2O_2+X,t}}{v_{Isom.} + \sum_{X=NO/RO_2/HO_2} v_{CH_3SCH_2O_2+X,t}} \quad (R5)$$

$$C_{Isom.t} = \frac{v_{Isom.}}{v_{Isom.} + \sum_{X=NO/RO_2/HO_2} v_{CH_3SCH_2O_2+X,t}} \quad (R6)$$

$$\text{Percentage of } CH_3SCH_2O_2\text{+X' channel} = \frac{\sum_{t=0} C_{CH_3SCH_2O_2+X,t}[CH_3SCH_2O_2]_t}{\sum_{t=0} C_{Isom.t}[CH_3SCH_2O_2]_t + \sum_{X=NO/RO_2/HO_2} (\sum_{t=0} C_{CH_3SCH_2O_2+X,t}[CH_3SCH_2O_2]_t} \quad (R7)$$

$$\text{Percentage of Isom.' channel} = \frac{\sum_{t=0} C_{Isom.t}[CH_3SCH_2O_2]_t}{\sum_{t=0} C_{Isom.t}[CH_3SCH_2O_2]_t + \sum_{X=NO/RO_2/HO_2} (\sum_{t=0} C_{CH_3SCH_2O_2+X,t}[CH_3SCH_2O_2]_t} \quad (R8)$$

$$\text{Amount of Isom.} = \sum_{t=0} C_{CH_3SCH_2O_2+X,t}[CH_3SCH_2O_2]_t \quad (R9)$$

where X denotes the concentration of NO, RO_2, or HO_2 (molecule cm^{-3}) at time t fitted by the MCM model in each experiment. $v_{CH3SCH2O2+X,t}$ denotes the rate (s^{-1}) at which the bimolecular reaction ($CH_3SCH_2O_2$ + $NO/RO_2/HO_2$) at time t, respectively. $k_{CH3SCH2O2+X}$ denotes the rate constant (molecule cm^{-3} s^{-1}) for the reaction of the $CH_3SCH_2O_2$ radical with NO, RO_2 or HO_2 at time t, respectively. The rate constants are respectively (Jacob et al., 2024): $k_{CH3SCH2O2+NO}$ = 1.169 × 10^{-10} molecule cm^{-3} s^{-1}, $k_{CH3SCH2O2+RO2}$ = 3.740 × 10^{-12} molecule cm^{-3} s^{-1}, $k_{CH3SCH2O2+HO2}$ = 5.805 × 10^{-12} molecule cm^{-3} s^{-1}. $v_{Isom.}$ is a constant, here assumed to be 0.06 s^{-1} (Jacob et al., 2024; Assaf et al., 2023). $C_{CH3SCH2O2+X,t}$ (%) denotes the rate percentage of the three bimolecular reaction channels at time t. $C_{Isom.t}$ (%) denotes the rate percentage of the isomerization reaction channel. $[CH_3SCH_2O_2]_t$ (molecule cm^{-3}) denotes the concentration of $CH_3SCH_2O_2$ radical at moment t. The percentage of $CH_3SCH_2O_2$ + X'channel or Isom.'channel (%) indicates the relative percentage of a particular bimolecular or isomerization reaction channel throughout the whole reaction process. Amount of Isom. (molecule cm^{-3}) denotes the absolute amount of the isomerization channel throughout the reaction process.

The simulation results are shown in Fig. R4 below. It can be found that the amount of the isomerization channel increases and then decreases as the ratio of precursor consumption increases. The increase in OHR mentioned in the manuscript leads to a decreasing trend of SOA yield after the turning point. This is directly supported by the amount of the isomerization channel of the model-fitted $CH_3SCH_2O_2$ radical. As the

Δ[DMS]/Δ[α-pinene] increases further, the absolute amount of isomerization decreases and OH regeneration is less significant.

This estimation result agrees with the measured SOA mass concentration, SOA yield, and OH concentration trends showing in Fig. 4, with the turning point at the Δ[DMS]/Δ[α-pinene] ratio of ~0.6 - 1 (i.e., Exp. AD-3 or AD-4). The slight difference (i.e., turning point at AD-3 vs AD-4) is likely due to the incomplete mechanism for DMS in the MCM model. Nevertheless, the results here suggest that the isomerization reaction intensity controls the OH concentration and therefore SOA formation in the mixed experiments.

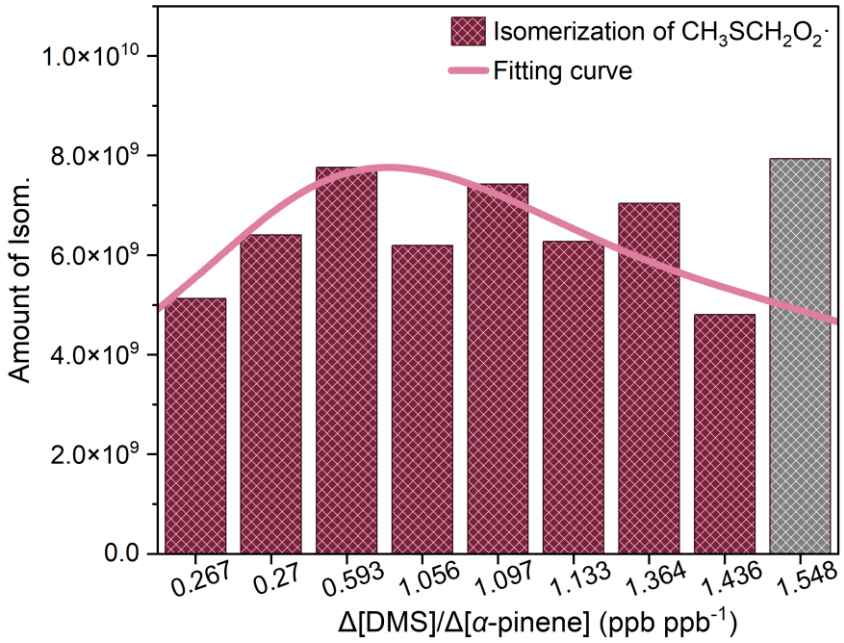

Figure R4. Amount of isomerization channels of $CH_3SCH_2O_2$ radical. A curve was drawn as a guide to the eye. The curve was fitted without using the last data point since it was much higher than the other points.

R1-5:) The proposed mechanisms in Figures 8 and 10 are flawed. The proposed isomerization reactions and H-shift do not occur in the atmosphere (Xu et al., 2019; Vereecken and Nozière, 2020).

A1-5:) Thank you for your valuable suggestion. We agree that the H-shift path shown in Fig. 8 from the original manuscript indeed cannot occur after reviewing the literature. We have removed the second pathway in Fig. 8 from the original manuscript after revision. At the same time, we have modified the first pathway to other pathways, while proposing $C_{10}H_{15}NO_6$ to be the other isomer. The molecular structure of the modified $C_{10}H_{15}NO_6$ is a ring-opening product, which is oxidized from pinonaldehyde (Eddingsaas et al., 2012a). In addition, we retained the molecular structure of the dimer $C_{20}H_{33}NO_8$, which is derived from Draper et al. (2015). The following texts and figures were added in the revised manuscript.

"Figure 12b shows the possible pathway of ON formation. In the presence of NO_2, the hydrogen atoms on the carbon chain of the typical product pinonaldehyde can be readily oxidized to form nitrogen-containing carboxylate products by the addition of oxygen, i.e., $C_{10}H_{15}NO_6$ (MW 245) (Boyd et al., 2015; Kim et al., 2012; Eddingsaas et al., 2012b)." (Page 20, Lines 417-420)

"In addition, Fig. 12b demonstrates the possible structure of a high molecular weight oligomer generated in the individual α-pinene experiments: $C_{20}H_{33}NO_8$ (MW 415). It is speculated that RO_2 tends more towards isomerization processes such as autoxidation compared to fragmentation reaction (Draper et al., 2015). This pathway increases the possibility of oligomerization of $RO_2 + RO_2$ and $RO_2 + HO_2$ in individual α-pinene oxidation." (Page 20, Lines 423-426)

The mechanisms related to ONs have also been modified, as shown below (Page 21, Lines 427-430).

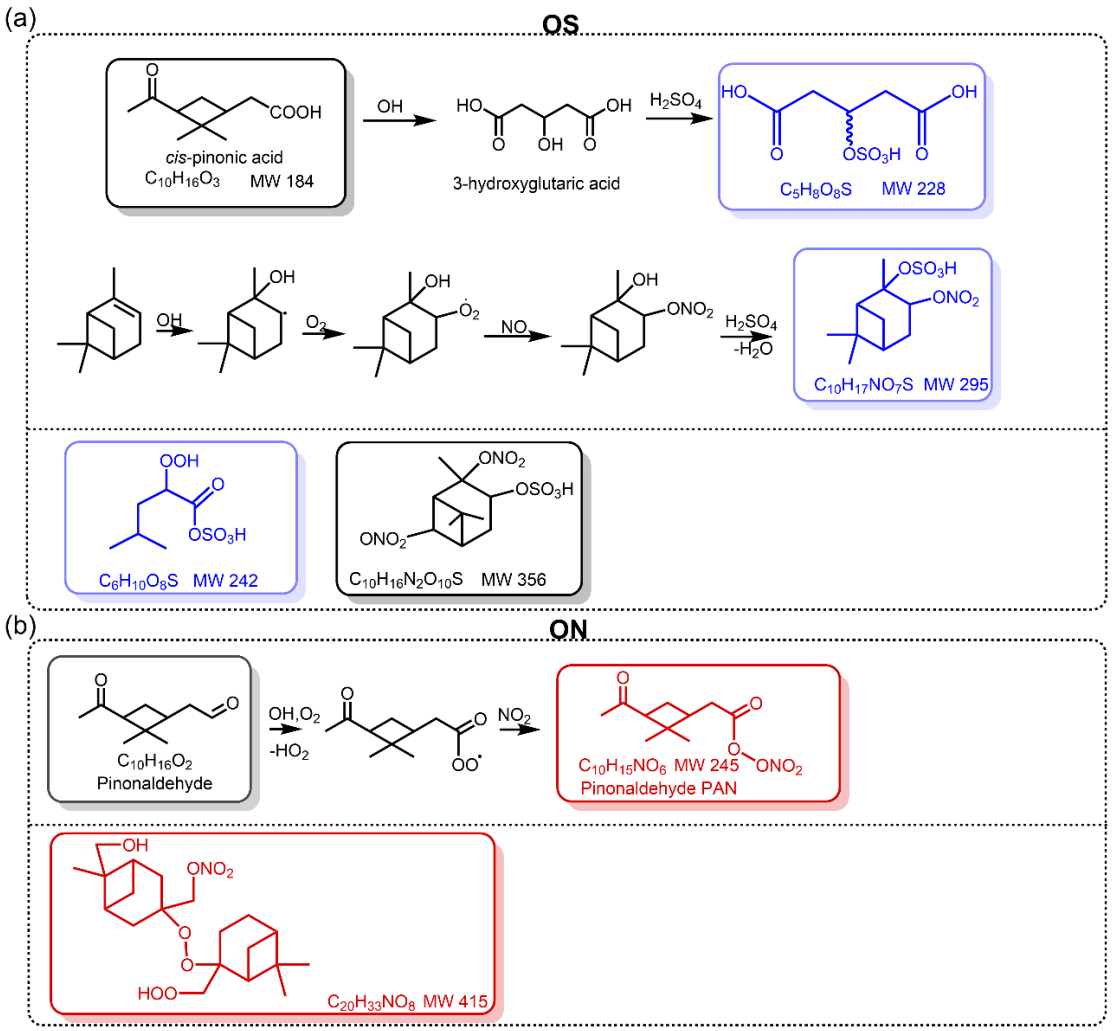

Figure 12. Proposed formation mechanisms and structural for organosulfate (a) and organic nitrates (b) in SOA. Red, blue and black in the boxes refer to the products identified by α-pinene-only SOA products, mixed-only SOA products and α-pinene-mixed-both SOA products, respectively.

We have combined Fig. 9, 10, and 11 from the original manuscript and modified the relevant textual content. The most direct effect of DMS on α-pinene SOA is the generation of sulfur-containing molecules. The fragmentation product $C_5H_8O_8S$ can be generated from pinonic acid. This has been demonstrated in Surratt et al. (2008). For $C_{10}H_{17}NO_7S$, we have modified it based on Wang et al. (2020). This product forms RO_2 by addition of OH and O_2. Then ON is formed in the presence of NO, followed by esterification by sulfuric acid to form the final product. As for $C_{10}H_{16}N_2O_{10}S$ and $C_6H_{10}O_8S$, we also found their presence in the studies of Surratt et al. (2008) and Xu et al. (2020). The relevant mechanisms of OS are shown in Fig. 12(a) above. The following texts were added in the revised manuscript.

"Acidic products of DMS can participate in the formation of α-pinene SOA. Acidic products are mainly generated by the H-abstraction pathway via photooxidation of DMS. At room temperature, H abstraction is the main reaction pathway, accounting for ~70% of the total reaction (Barnes et al., 2006). As shown in Fig. 1, this pathway first generates the CH_3SCH_2 radical, which can add to O_2 to generate the $CH_3SCH_2O_2$ radical, followed by reaction with RO_2 or HO_2 to generate peroxy hydroxyl or peroxy nitrate, or with NO, eventually generating SO_2, MSA and H_2SO_4. In the composition analysis of SOA generated by photooxidation of DMS-α-pinene, a number of sulfur-containing compounds were generated. Based on previous studies (Aschmann et al., 2002; Surratt et al., 2008; Surratt et al., 2007; Gao et al., 2006), we identify some potential OSs (Table S4). Figure 12a shows the reaction pathway for C_5 OS generation. The oxidation product, pinonic acid reacts with OH to form 2/3-hydroxyglutaric acid (3-Hydroxyglutaric acid as an example) under high-NO condition, followed by sulfation to form $C_5H_8O_8S$ (MW 228) (Surratt et al., 2008). Xu et al. (2020) detected the isomer of $C_6H_{10}O_8S$ (MW 242), which was speculated to be a fragmentation product formed by further oxidation by ring structure breakage during the reaction." (Page 20, Lines 396-406)

"Due to the presence of NO_x, we detected monomer compounds containing nitrogen-containing OSs (NOSs) which can demonstrate the coexistence of nitrate and sulfate groups. Figure 12a shows the reaction pathway for one of C_{10} NOS generation. $C_{10}H_{17}NO_7S$ is formed by heterogeneous reactions of SO_2 with intermediates. The pathway usually occurs in the particle phase (Wang et al., 2020). Surratt et al. (2008) had identified the $C_{10}H_{16}N_2O_{10}S$ (MW 356) product and proposed that it would form in the presence of highly acidic seeds that produces hydroperoxides containing two nitro groups firstly, which further eliminate one water molecule by sulfation. Combined with Table S4, the changes in the relative abundance of the majority of OSs in different mixing systems are consistent with the pattern of change in the yield of mixed SOA. This phenomenon suggests that DMS is most likely to influence the mechanism of α-pinene SOA production through acidic products, especially the contribution of the C_{10} NOSs." (Page 20, Lines 407-415)

We have found that DMS also affects the CHO molecules of α-pinene SOA. We have speculated on the mechanisms of formation of some CHO molecules. This part was presented in Sect. S8, Fig. S9 and Fig. S10 of the original supplement. We selected

representative substances therein, mainly highly oxygenated organic molecules of C_8 - C_{10}. They are $C_8H_{12}O_4$, $C_7H_{10}O_4$, $C_{10}H_{16}O_2$, $C_{10}H_{16}O_3$, $C_{10}H_{16}O_4$, $C_9H_{14}O_4$, $C_9H_{14}O_6$, $C_8H_{12}O_3$, $C_9H_{14}O_5$, $C_8H_{12}O_6$, and $C_8H_{12}O_5$, respectively. These products represent *α*-pinene-only SOA products, mixed-only SOA products and *α*-pinene-mixed-both SOA products, respectively. Among them, the three products, $C_{10}H_{16}O_4$, $C_9H_{14}O_6$, and $C_8H_{12}O_5$, have similar trends in the variation of yield in different systems.

The following texts and figure were added in the revised manuscript.

"The effect of DMS on the formation of *α*-pinene SOA is multiple. Table S4 shows some typical substances in different oxidation systems. The addition of DMS resulted in the generation of more C_8 - C_{10} HOMs in the *α*-pinene SOA. Based on the previous studies (Librando and Tringali, 2005; Kristensen et al., 2014; Yasmeen et al., 2010; Aschmann et al., 1998; Gao et al., 2006), we showed the possible formation pathways of some of these typical CHO molecules in Fig. 11. In the presence of NO_x, *α*-pinene undergoes OH addition and oxidation to form RO_2. In the first pathway, this first-generational RO_2 undergoes multigenerational autoxidation or reacts with NO to form terpenylic acid ($C_8H_{12}O_4$, MW 172). Terpenylic acid has the highest relative abundance in the product of *α*-pinene SOA compared to the mixed systems. Therefore, in an individual system, terpenylic acid is more likely to undergo further oxidation to produce terebic acid ($C_7H_{10}O_4$, MW 158), which proves the view of Claeys et al. (2009) that the onset of terebic aldehyde oxidation is assumed to be in the particle phase, and this substance contributes dominantly to the particle phase product in individual *α*-pinene oxidation." (Pages 17-18, Lines 373-382)

"In the second pathway, the first-generational RO_2 can interact with NO to form RO, which can undergo isomerization and other processes to form pinonaldehyde ($C_{10}H_{16}O_2$, MW 168). Pinonaldehyde can be accompanied by the generation of HO_2, and then further oxidized to hydroperoxide ($C_{10}H_{16}O_4$, MW 200) and *cis*-pinonic acid ($C_{10}H_{16}O_3$, MW 184), which is a typical gas-phase product. *cis*-Pinonic acid can produce RO_2 containing several functional groups, which forms pinic acid ($C_9H_{14}O_4$, MW 186) in the presence of NO and HO_2. Further oxidation of pinic acid can form RO_2, which undergoes reactions such as isomerization, dissociation to form a number of monomer compounds of C_8 and C_9 in the particle phase, including the HOMs such as $C_9H_{14}O_6$ (MW 218), $C_9H_{14}O_5$ (MW 202), $C_8H_{12}O_3$ (MW 156). $C_8H_{12}O_3$ oxidized by chain termination to from $C_8H_{12}O_5$ (MW 188) and $C_8H_{12}O_6$ (MW 204). Overall, the addition of DMS promotes a deeper oxidation of the intermediate product generated by the oxidation of *α*-pinene, as reflected in the opening of the six-membered ring, resulting in the formation of a multifunctional peroxycarboxylic acid." (Pages 18-19, Lines 383-392)

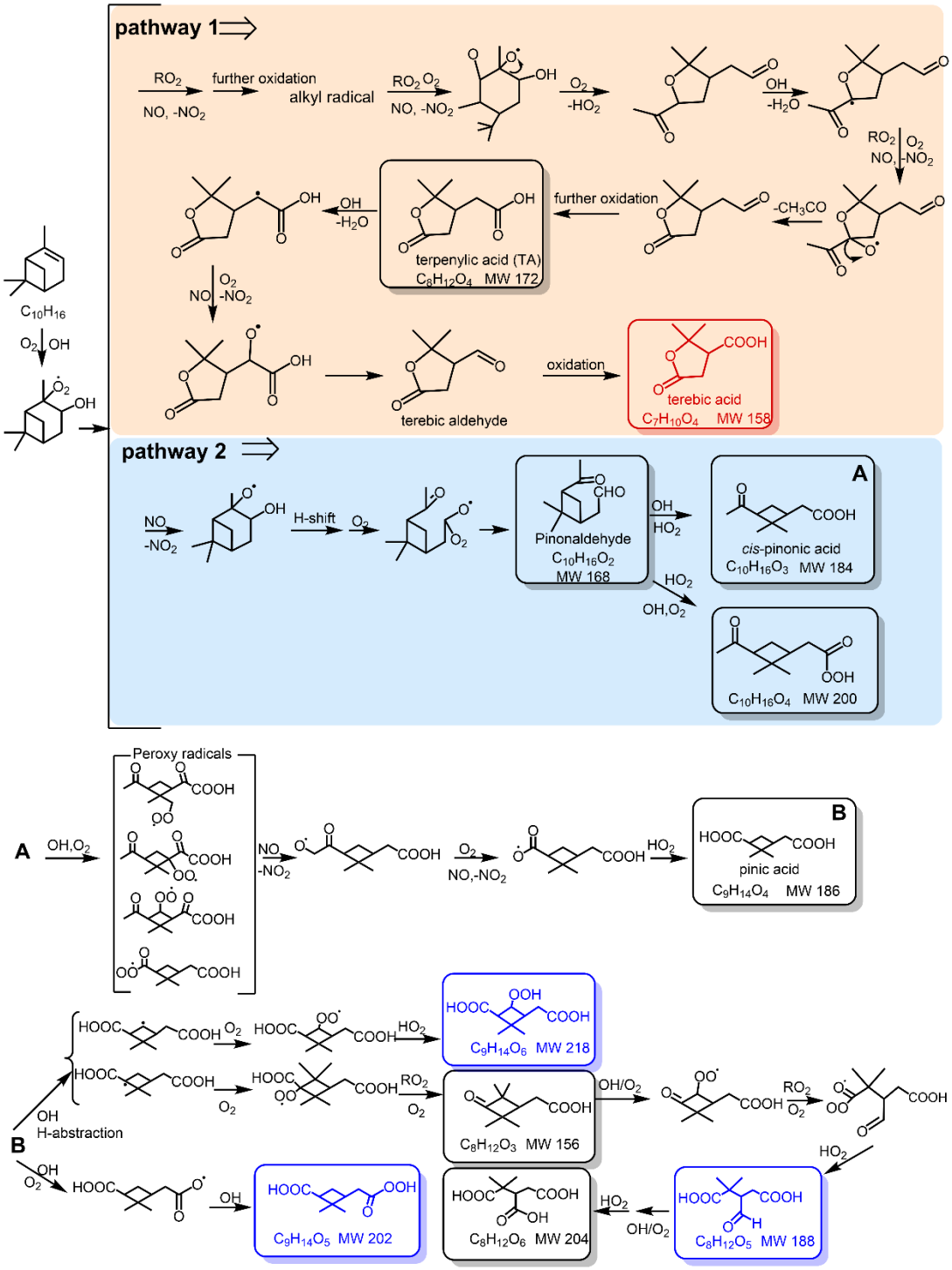

Figure 11. Proposed formation mechanisms and structural for CHO molecules in SOA. Red, blue and black in the boxes refer to the products identified by α-pinene-only SOA products, mixed-only SOA products and α-pinene-mixed-both SOA products, respectively.

Subsequently, we also proposed the mechanisms for the other CHO products in the text of the revised supplement.

"Several other CHO compounds were also generated in different systems. Based on the previous studies (Librando and Tringali, 2005; Kristensen et al., 2014; Yasmeen

et al., 2010; Aschmann et al., 1998; Gao et al., 2006), we sorted out the possible formation mechanisms of the products of individual *α*-pinene and mixed oxidation in our experiments, as shown in Fig. S9. Figure S9 illustrates the four photooxidation pathways of *α*-pinene. *α*-Pinene forms RO_2 under the oxidation of OH and O_2, and further forms RO in the presence of RO_2 or NO. The six-membered ring of RO opens, removing a CH_3 fragment molecule to form the product, namely $C_9H_{14}O_3$ (MW 170). Further oxidation of the gas-phase typical product, pinic acid, leads to the formation of $C_8H_{12}O_3$ (MW 156). This product undergoes the action of O_2 to form RO_2, which passes through the RO_2 + HO_2 channel to form the final product, $C_8H_{12}O_4$ (MW 172). In addition to generating hydroperoxide ($C_{10}H_{16}O_4$, MW 200) and *cis*-pinonic acid ($C_{10}H_{16}O_3$, MW 184) as mentioned in the Section 3.3.2, the intermediate product pinonaldehyde can be oxidized to form $C_9H_{14}O_2$ (MW 154) and $C_{10}H_{18}O_3$ (MW 186)." (SI Page 10, Lines 205-214)

"Figure S9 also shows other products formed by the oxidation of the gas-phase product *cis*-pinonic acid ($C_{10}H_{16}O_3$, MW 184) besides the products in Fig. 11, which forms a number of peroxyl radicals in the presence of OH or O_2, and the subsequent reactions of these peroxyl radicals can be divided into four pathways." (SI Page 10, Lines 215-217)

Revised possible reaction pathway of CHO products is showed as Fig. S9 in the supplement (SI Page 17, Lines 270-272).

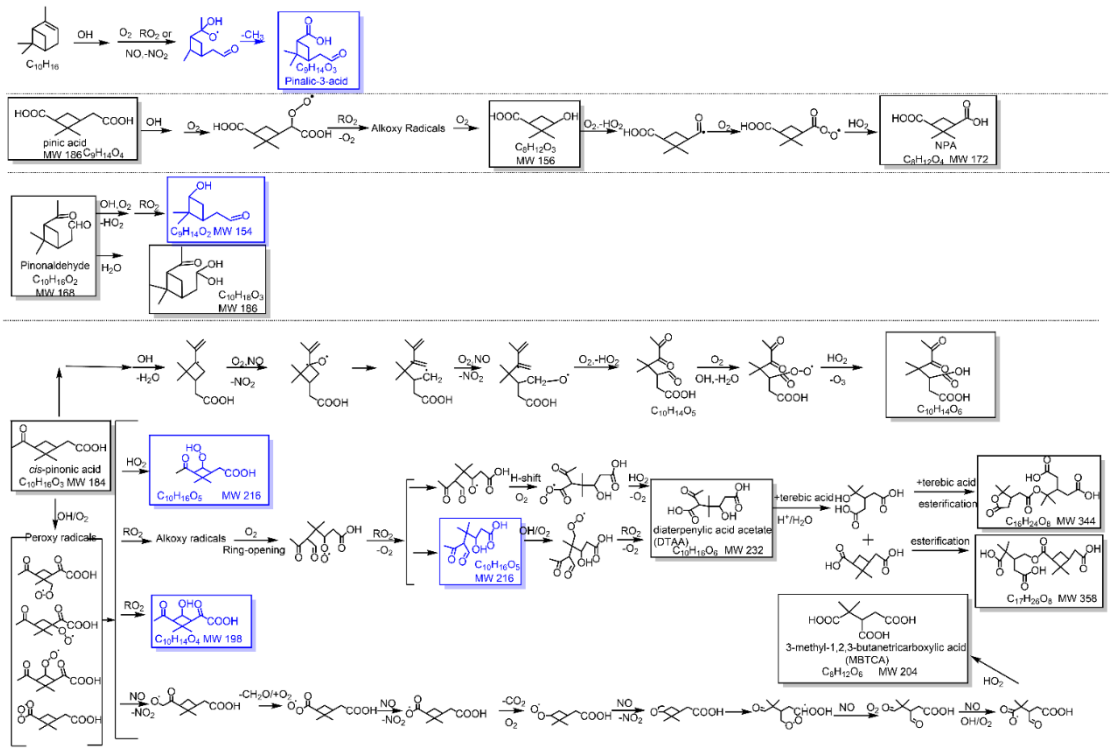

Figure S9. Possible reaction pathway of CHO products generation. Blue and black in the boxes refer to the product identified by mixed-only SOA products and *α*-pinene-mixed-both SOA products, respectively.

Minor Comments:

R1-6:) The head row of Table 3 is confusing. The table seems to have two different head rows. For example, does the first column correspond to [total particles] or delta[α-pinene]?

A1-6:) Thank you for your valuable suggestion. We have modified the head row of Table 3 (now Table 2 in the revised manuscript).

Page 9, Line 198 in the revised manuscript. As follows:

Table 2. Experimental results of particle-phase components in photooxidation of DMS/α-pinene/NO_x systems.

Exp. No.	[Total particles] [a] μg m^{-3}	[H_2SO_4][b] μg m^{-3}	[MSA][b] μg m^{-3}	[SOA_m][c] μg m^{-3}	Y_m[d]	[SOA_p][e] μg m^{-3}
individual α-pinene						
A-1	269.5	-	-	269.5	0.16±0.02	
individual DMS						
D-1	177.2	50.8	32.83	116.2	0.25±0.03	
mix α-pinene and DMS						
AD-1	296.3	15.0	22.2	270.8	0.14±0.02	216.7
AD-2	422.3	15.7	22.5	400.1	0.20±0.02	270.3
AD-3	572.6	45.4	24.9	507.5	0.24±0.02	425.8
AD-4	714.4	55.4	50.5	607.7	0.25±0.03	648.7
AD-5	683.0	48.8	36.2	613.1	0.24±0.02	708.2
AD-6	551.5	35.3	8.5	504.2	0.19±0.02	680.9
AD-7	539.9	48.4	16.8	476.0	0.19±0.02	677.5
AD-8	364.4	68.7	0.1	237.1	0.08±0.01	537.6
AD-9	289.9	83.2	7.0	154.0	0.06±0.01	436.5

[a] The mass concentration of particles generated by SMPS, corrected for particle wall loss, was calculated as a particle density of 1.2 g cm^{-3}.

[b] IC detection, particle-phase products generated by DMS photooxidation. NH_4^+ was hardly detected. All SO_4^{2-} were detected by IC as H_2SO_4.

[c] The measured SOA mass concentration is expressed as $[\text{Total particles}]_{\text{after-correction}} \times (1 - [H_2SO_4] / [\text{Total particles}]_{\text{before-correction}})$.

[d] $[SOA_m] / (\Delta[\alpha\text{-pinene}] + \Delta[\text{DMS}])$, as mixed yield. Error bars indicate SMPS instrument error of 10%.

[e] The predicted SOA mass concentration by using mass-dependent SOA yields of α-pinene and DMS.

R1-7:) Describe how the volatility of each compound is estimated for Figure 6.

A1-7:) Thank you for your valuable suggestion. We showed how to assess the volatility of each compound in the supplement. The following texts were added in the revised manuscript.

"The volatility calculation for all the components are shown in Sect. S4." (Page 15, Lines 332-333)

R1-8:) Line 3. Grammar error. I assume what the authors want to express is that “OH generation before the turning point could attribute to the enhancement in SOA formation.”

A1-8:) Thank you for your valuable suggestion. The following texts were revised in the new manuscript.

“OH regeneration before the turning point could attribute to the enhancement in SOA formation.” (Page 12, Lines 250-251)

References:

Aschmann, S. M., Atkinson, R., and Arey, J.: Products of reaction of OH radicals with α-pinene, J. Geophys. Res., 107, ACH 6-1-ACH 6-7, 10.1029/2001JD001098, 2002.

Aschmann, S. M., Reisseil, A., Atkinson, R., and Arey, J.: Products of the gas phase reactions of the OH radical with α- and β-pinene in the presence of NO, J. Geophys. Res., 103, 25553-25561, 10.1029/98JD01676, 1998.

Assaf, E., Finewax, Z., Marshall, P., Veres, P. R., Neuman, J. A., and Burkholder, J. B.: Measurement of the intramolecular hydrogen-shift rate coefficient for the CH_3SCH_2OO radical between 314 and 433 K, J. Phys. Chem. A, 127, 2336-2350, 10.1021/acs.jpca.2c09095, 2023.

Barnes, I., Hjorth, J., and Mihalopoulos, N.: Dimethyl sulfide and dimethyl sulfoxide and their oxidation in the atmosphere, Chem. Rev., 106, 940-975, 10.1021/cr020529+, 2006.

Berndt, T., Hoffmann, E. H., Tilgner, A., Stratmann, F., and Herrmann, H.: Direct sulfuric acid formation from the gas-phase oxidation of reduced-sulfur compounds, Nat. Commun., 14, 4849, 10.1038/s41467-023-40586-2, 2023.

Berndt, T., Chen, J., Møller, K. H., Hyttinen, N., Prisle, N. L., Tilgner, A., Hoffmann, E. H., Herrmann, H., and Kjaergaard, H. G.: SO_2 formation and peroxy radical isomerization in the atmospheric reaction of OH radicals with dimethyl disulfide, Chem. Comm., 56, 13634-13637, 10.1039/D0CC05783E, 2020.

Boyd, C. M., Sanchez, J., Xu, L., Eugene, A. J., Nah, T., Tuet, W. Y., Guzman, M. I., and Ng, N. L.: Secondary organic aerosol formation from the β-pinene + NO_3 system: Effect of humidity and peroxy radical fate, Atmos. Chem. Phys., 15, 7497-7522, 10.5194/acp-15-7497-2015, 2015.

Chen, J., Berndt, T., Møller, K. H., Lane, J. R., and Kjaergaard, H. G.: Atmospheric fate of the CH_3SOO radical from the $CH_3S + O_2$ equilibrium, J. Phys. Chem. A, 125, 8933-8941, 10.1021/acs.jpca.1c06900, 2021.

Claeys, M., Iinuma, Y., Szmigielski, R., Surratt, J. D., Blockhuys, F., Van Alsenoy, C., Böge, O., Sierau, B., Gómez-González, Y., Vermeylen, R., Van der Veken, P., Shahgholi, M., Chan, A. W. H., Herrmann, H., Seinfeld, J. H., and Maenhaut, W.: Terpenylic acid and related compounds from the oxidation of α-pinene: Implications for new particle formation and growth above forests, Environ. Sci. Technol., 43, 6976-6982, 10.1021/es9007596, 2009.

Coates, J. and Butler, T. M.: A comparison of chemical mechanisms using tagged ozone production potential (TOPP) analysis, Atmos. Chem. Phys., 15, 8795-8808, 10.5194/acp-15-8795-2015, 2015.

Draper, D. C., Farmer, D. K., Desyaterik, Y., and Fry, J. L.: A qualitative comparison of secondary organic aerosol yields and composition from ozonolysis of monoterpenes at varying concentrations of NO_2, Atmos. Chem. Phys., 15, 12267-12281, 10.5194/acp-15-12267-2015, 2015.

Eddingsaas, N. C., Loza, C. L., Yee, L. D., Seinfeld, J. H., and Wennberg, P. O.: α-Pinene photooxidation under controlled chemical conditions – Part 1: Gas-phase composition in low- and high-NO_x environments, Atmos. Chem. Phys., 12, 6489-6504, 10.5194/acp-12-6489-2012, 2012a.

Eddingsaas, N. C., Loza, C. L., Yee, L. D., Chan, M., Schilling, K. A., Chhabra, P. S., Seinfeld, J. H., and Wennberg, P. O.: α-Pinene photooxidation under controlled chemical conditions – Part 2: SOA yield and composition in low- and high-NO_x environments, Atmos. Chem. Phys., 12, 7413-7427, 10.5194/acp-12-7413-2012, 2012b.

Gao, S., Surratt, J. D., Knipping, E. M., Edgerton, E. S., Shahgholi, M., and Seinfeld, J. H.: Characterization of polar organic components in fine aerosols in the southeastern United States: Identity, origin, and evolution, J. Geophys. Res., 111, D14314, 10.1029/2005JD006601, 2006.

Jacob, L. S. D., Giorio, C., and Archibald, A. T.: Extension, development, and evaluation of the representation of the OH-initiated dimethyl sulfide (DMS) oxidation mechanism in the Master Chemical Mechanism (MCM) v3.3.1 framework, Atmos. Chem. Phys., 24, 3329-3347, 10.5194/acp-24-3329-2024, 2024.

Jernigan, C. M., Fite, C. H., Vereecken, L., Berkelhammer, M. B., Rollins, A. W., Rickly, P. S., Novelli, A., Taraborrelli, D., Holmes, C. D., and Bertram, T. H.: Efficient production of carbonyl sulfide in the low-NO_x oxidation of dimethyl sulfide, Geophys. Res. Lett., 49, e2021GL096838, 10.1029/2021GL096838, 2022.

Kim, H., Barkey, B., and Paulson, S. E.: Real refractive indices and formation yields of secondary organic aerosol generated from photooxidation of limonene and α-pinene: The effect of the HC/NO_x ratio, J. Phys. Chem. A, 116, 6059–6067, 10.1021/jp301302z.s001, 2012.

Knote, C., Tuccella, P., Curci, G., Emmons, L., Orlando, J. J., Madronich, S., Baró, R., Jiménez-Guerrero, P., Luecken, D., Hogrefe, C., Forkel, R., Werhahn, J., Hirtl, M., Pérez, J. L., San José, R., Giordano, L., Brunner, D., Yahya, K., and Zhang, Y.: Influence of the choice of gas-phase mechanism on predictions of key gaseous pollutants during the AQMEII phase-2 intercomparison, Atmos. Environ., 115, 553-568, 10.1016/j.atmosenv.2014.11.066, 2015.

Kristensen, K., Cui, T., Zhang, H., Gold, A., Glasius, M., and Surratt, J. D.: Dimers in α-pinene secondary organic aerosol: Effect of hydroxyl radical, ozone, relative humidity and aerosol acidity, Atmos. Chem. Phys., 14, 4201-4218, 10.5194/acp-14-4201-2014, 2014.

Librando, V. and Tringali, G.: Atmospheric fate of OH initiated oxidation of terpenes. Reaction mechanism of α-pinene degradation and secondary organic aerosol formation, J. Environ. Manage., 75, 275-282, 10.1016/j.jenvman.2005.01.001, 2005.

Lv, G., Zhang, C., and Sun, X.: Understanding the oxidation mechanism of methanesulfinic acid by ozone in the atmosphere, Sci. Rep., 9, 322, 10.1038/s41598-018-36405-0, 2019.

Odum, J. R., Hoffmann, T., Bowman, F., Collins, D., Flagan, R. C., and Seinfeld, J. H.: Gas/Particle partitioning and Secondary Organic Aerosol Yields, Environ. Sci. Technol., 30, 2580-2585, 10.1021/es950943+, 1996.

Pankow, J. F.: An absorption model of gas/particle partitioning of organic compounds in the atmosphere, Atmos. Environ., 28, 185-188, 10.1016/1352-2310(94)90093-0, 1994.

Surratt, J. D., Kroll, J. H., Kleindienst, T. E., Edney, E. O., Claeys, M., Sorooshian, A., Ng, N. L., Offenberg, J. H., Lewandowski, M., Jaoui, M., Flagan, R. C., and Seinfeld, J. H.: Evidence for organosulfates in secondary organic aerosol, Environ. Sci. Technol., 41, 517-527, 10.1021/es062081q, 2007.

Surratt, J. D., Gómez-González, Y., Chan, A. W. H., Vermeylen, R., Shahgholi, M., Kleindienst, T. E., Edney, E. O., Offenberg, J. H., Lewandowski, M., Jaoui, M., Maenhaut, W., Claeys, M., Flagan, R. C., and Seinfeld, J. H.: Organosulfate formation in biogenic secondary organic aerosol, J. Phys. Chem. A, 112, 8345-8378, 10.1021/jp802310p, 2008.

Vereecken, L. and Nozière, B.: H migration in peroxy radicals under atmospheric conditions, Atmos. Chem. Phys., 20, 7429-7458, 10.5194/acp-20-7429-2020, 2020.

Veres, P. R., Neuman, J. A., Bertram, T. H., Assaf, E., Wolfe, G. M., Williamson, C. J., Weinzierl, B., Tilmes, S., Thompson, C. R., Thames, A. B., Schroder, J. C., Saiz-Lopez, A., Rollins, A. W., Roberts, J. M., Price, D., Peischl, J., Nault, B. A., Møller, K. H., Miller, D. O., Meinardi, S., Li, Q., Lamarque, J.-F., Kupc, A., Kjaergaard, H. G., Kinnison, D., Jimenez, J. L., Jernigan, C. M., Hornbrook, R. S., Hills, A., Dollner, M., Day, D. A., Cuevas, C. A., Campuzano-Jost, P., Burkholder, J., Bui, T. P., Brune, W. H., Brown, S. S., Brock, C. A., Bourgeois, I., Blake, D. R., Apel, E. C., and Ryerson, T. B.: Global airborne sampling reveals a previously unobserved dimethyl sulfide oxidation mechanism in the marine atmosphere, Proc. Natl. Acad. Sci., 117, 4505-4510, 10.1073/pnas.1919344117, 2020.

Wang, Y., Hu, M., Wang, Y. C., Li, X., Fang, X., Tang, R., Lu, S., Wu, Y., Guo, S., Wu, Z., Hallquist, M., and Yu, J. Z.: Comparative study of particulate organosulfates in contrasting atmospheric environments: Field evidence for the significant influence of anthropogenic sulfate and NO_x, Environ. Sci. Technol. Lett., 7, 787-794, 10.1021/acs.estlett.0c00550, 2020.

Xu, L., Møller, K. H., Crounse, J. D., Otkjær, R. V., Kjaergaard, H. G., and Wennberg, P. O.: Unimolecular reactions of peroxy radicals formed in the oxidation of α-pinene and β-pinene by hydroxyl radicals, J. Phys. Chem. A, 123, 1661-1674, 10.1021/acs.jpca.8b11726, 2019.

Xu, L., Tsona, N. T., You, B., Zhang, Y., Wang, S., Yang, Z., Xue, L., and Du, L.: NO_x enhances secondary organic aerosol formation from nighttime γ-terpinene ozonolysis, Atmos. Environ., 225, 117375, 10.1016/j.atmosenv.2020.117375, 2020.

Yang, X., Yuan, B., Peng, Z., Peng, Y., Wu, C., Yang, S., Li, J., and Shao, M.: Inter-comparisons of VOC oxidation mechanisms based on box model: A focus on OH reactivity, J. Environ. Sci., 114, 286-296, 10.1016/j.jes.2021.09.002, 2022.

Yasmeen, F., Vermeylen, R., Szmigielski, R., Iinuma, Y., Böge, O., Herrmann, H., Maenhaut, W., and Claeys, M.: Terpenylic acid and related compounds: precursors for dimers in secondary organic aerosol from the ozonolysis of α- and β- pinene, Atmos. Chem. Phys., 10, 9383-9392, 10.5194/acp-10-9383-2010, 2010.

Ye, Q., Goss, M. B., Krechmer, J. E., Majluf, F., Zaytsev, A., Li, Y., Roscioli, J. R., Canagaratna, M., Keutsch, F. N., Heald, C. L., and Kroll, J. H.: Product distribution, kinetics, and aerosol formation from the OH oxidation of dimethyl sulfide under different RO_2 regimes, Atmos. Chem. Phys., 22, 16003-16015, 10.5194/acp-22-16003-2022, 2022.

Zong, R., Xue, L., Wang, T., and Wang, W.: Inter-comparison of the regional atmospheric chemistry mechanism (RACM2) and master chemical mechanism (MCM) on the simulation of acetaldehyde, Atmos. Environ., 186, 144-149, 10.1016/j.atmosenv.2018.05.013, 2018.